Magnetic Resonance in Medicine 41:964–972 (1999)

Motion Correction in fMRI via Registration of Individual Slices Into an Anatomical Volume

Boklye Kim,* Jennifer L. Boes, Peyton H. Bland, Thomas L. Chenevert, and Charles R. Meyer

An automated retrospective image registration based on mutual information is adapted to a multislice functional magnetic resonance imaging (fMRI) acquisition protocol to provide accurate motion correction. Motion correction is performed by mapping each slice to an anatomic volume data set acquired in the same fMRI session to accommodate inter-slice head motion. Accuracy of the registration parameters was assessed by registration of simulated MR data of the known truth. The widely used rigid body volume registration approach based on stacked slices from the time series data may hinder statistical accuracy by introducing inaccurate assumptions of no motion between slices for multislice fMRI data. Improved sensitivity and specificity of the fMRI signal from mapping-each-slice-to-volume method is demonstrated in comparison with a stacked-slice correction method by examining functional data from two normal volunteers. The data presented in a standard anatomical coordinate system suggest the reliability of the mapping-each-slice-to-volume method to detect the activation signals consistent between the two subjects. Magn Reson Med 41:964–972, 1999.

Key words: fMRI; motion correction; registration; mapping; MI; mutual information; echoplanar imaging; EPI

Subject motion during time series functional magnetic resonance image (fMRI) acquisition alters voxel intensity and introduces motion artifacts unrelated to stimulus-induced signal changes. The most common subject head motions are nodding and side-to-side motion, which require out-of-plane motion correction as well as subsequent in-plane motion correction for axial images. Subject motion correction, therefore, should not be restricted to in-plane (1,2).

Most fMRI data are acquired via multislice single-shot echoplanar imaging (EPI) sequences, in which slices are acquired at sequential intervals. Retrospective motion correction has been applied by other investigators to correct the motion artifacts (1–4). Frequently, realignment of slice stacks is used for the motion correction of fMRI images from time series data (1). The slice-stack approach, e.g., registration of multislice fMRI data using three-dimensional (3D) volume transformation of a misaligned slice stack, is an inaccurate estimation of subject motion that is inherent in multislice EPI acquisition sequence since each slice is excited at a sequential time interval. A set of acquired slices from a moving volume cannot be stacked together in parallel to form a volume consistent with patient geometry. To account for movements during time intervals between contiguous slice acquisitions, it is important, although non-trivial, to register individual slices into a high-resolution anatomical volume to reposition them to actual spatial locations. A motion correction using a *mapping-each-slice-into-volume*, e.g., *map-slice-to-volume*, approach is implemented to be adaptable to a multislice acquisition protocol.

In the *map-slice-to-volume* approach, individual slices acquired by a multislice single shot EPI are repositioned into an anatomical reference volume space and reconstructed into volume data. An accurate registration method is required for a precise spatial positioning of each slice for accurate statistical inference of the fMRI signal. An automated registration method based on mutual information has been shown to be effective for registration of functional and anatomical image data (5,6). Mutual information, a metric from classical information theory, is used for a mapping cost function to drive automatic registration and its robust nature allows accurate registration of an image pair without user-supplied information or preprocessing (7). A time series EPI data set of three to six activation cycles may contain 300–2000 slice images. An automated registration process is crucial for correction of each slice in such huge data sets.

Presented in this paper are *map-slice-to-volume* motion correction using rigid body transformation of six degrees of freedom (DOF), (i.e., rotation/translate) and the evaluation of the result in comparison with the slice-stack correction method. The effect of motion correction on activation signal analyses of fMRI data sets from two normal volunteers that reveal different severity in motion artifact is demonstrated.

MATERIALS AND METHODS

Image Acquisition

The functional MR image data presented in this section were acquired using a gradient-recalled echo (GRE) EPI sequence on a GE Signa system operating at field strength of 1.5 T. T_2*-weighted axial images were acquired of five 8 mm thick, contiguous slices, with a field of view (FOV) of 24 × 24 cm in a 64 × 64 matrix with the acquisition parameter TR/TE 2000/40 msec. In all, 20 images were acquired at each slice location. For an anatomical reference image, T_1-weighted MR volume image was acquired, in each fMRI experiment, following the fMRI session using a 3D spoiled GRASS (SPGR) sequence covering approximately the same volume as the fMRI data with a slice thickness of 2 mm and FOV of 24 × 24 cm in a 256 × 256 matrix.

For the sensory motor stimulation experiment, repetitive finger opposition tasks were performed by normal volunteers. For each run, a volunteer was asked to perform either

Department of Radiology, University of Michigan, Ann Arbor, Michigan.

Grant sponsor: DHHS NIH; Grant number: 2R01 CA59412–04A1.

*Correspondence to: Boklye Kim, Department of Radiology, University of Michigan Medical Center, Kresge III Box 0553, Ann Arbor, MI 48109–0553. E-mail: boklyek@umich.edu

Received 1 May 1998; revised 10 November 1998; accepted 20 November 1998.

uni- or bi- lateral sequential finger tapping for 20 sec on and 20 sec off. The tapping sequence was thumb with the digits 2–3-4–5 or, alternating sequence, 2–4-3–5.

Motion Correction Routine Using Automated Registration

A robust image registration is driven by the mutual information metric (MI), a mapping cost metric based on a classical information theory, and performs a six DOF rigid body transformation to reposition slices from fMRI time series data. The process is fully automated for motion correction of fMRI slices with respect to an anatomical reference volume acquired in the same fMRI acquisition session. The mutual information metric and Mutual Information Automated Multimodality Image Fusion (MIAMI Fuse) software were presented previously for spatial mapping of multimodal image data sets (5,6). A brief theoretical background is introduced below (8–10).

Mutual Information

Mutual information by definition, $I(x,y) = H(x) + H(y) - H(x,y)$, quantifies interdependency of two variables, e.g., image features such as gray scale intensities. $H(X)$, the entropy of a random variable, X, quantifies the average information required to describe X and is defined by $H(X) = -(p(x) \log p(x)$, where $p(x)$ is the probability density function of X; and $H(Y)$, in the same manner. Joint entropy, $H(X,Y)$, of a pair of random variables is defined by $H(X,Y) = -\Sigma\Sigma p(x,y) \log p(x,y)$, as a function of joint density probability, $p(x,y)$. By substituting gray level intensities, g_1 and g_2, for x and y, the joint gray scale density distribution function, $p(x,y)$, is constituted by scanning through all pixel pairs of geometrically mapped images to create a 2D histogram.

The mutual information metric, $MI = -I(x,y)$, is calculated from the joint density function, $p(x,y)$, of gray values of two geometrically mapped image sets. As defined mathematically (7),

$$I(X;\, Y) = \sum_{x \in X} \sum_{y \in Y} p(x, y) \log \frac{p(x, y)}{p(x)p(y)}$$

mutual information is a function of marginal and joint probability distributions, $p(x)$, $p(y)$, and $p(x,y)$, respectively. Mutual information by definition is bounded by complete independence ($I(X;Y) = 0$) and by one-to-one mapping ($I(X;X) = H(X)$); $0 \leq I(X;Y) \leq min(H(X),H(Y))$. The registration cost function, MI, can be obtained by normalizing $p(g_1,g_2)$, the 2D histogram of the gray values of the common pixels of the two images.

Dispersion in the 2D gray value scatter plot, $p(x,y)$, and thus joint entropy, of geometrically mapped pixel gray value pairs from a set of images is associated with (mis)registration. The dispersion is expected to be minimized when two images are registered. In Fig. 1, the 2D histograms are presented as intensity-modulated plots. The effect of (mis)registration of two images (top row) is depicted in the histograms, i.e., scatter plot, as a function of in-plane translation of 0, 1, 3, and 5 pixels in lateral direction (dx). Scatter plots were generated from two identical T_1-weighted MR images (Fig. 1; middle row) and a pair of T_1- and T_2- weighted MR images (Fig.1; bottom row) as the plots are indexed from the point of register

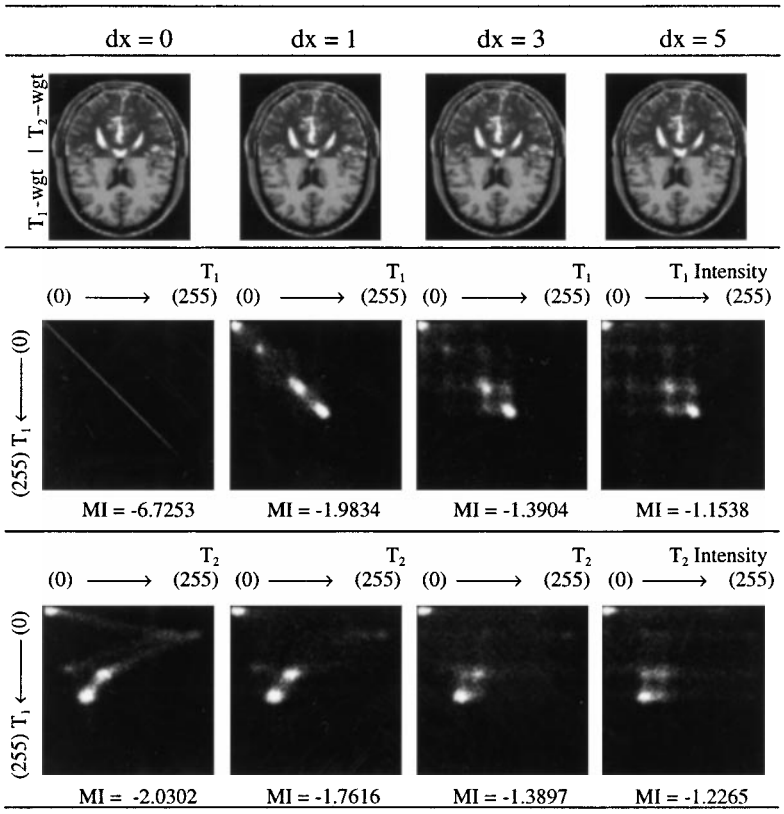

FIG. 1. Each row shows the effect of misregistration of the images as a function of lateral displacement of dx = 0, 1, 3, 5 pixels, where dx = 0 marks the position of the perfect registration. Top row: Top and bottom half images of T_2- and T_1-weighted MR images, respectively, at the same slice location. Middle and bottom rows: 2D gray scale histogram of an image pair, (middle) identical images, T_1-weighted, and (bottom) T_2- and T_1-weighted MR images. Top left corner of the 2D histograms indicates gray value intensity pair (0,0) and each axis is scaled from 0 to 255. For each 2D histogram, the corresponding MI cost metric is indicated.

(dx = 0) by in-plane translation. The left top corner indicates the origin (0,0) and the plots are scaled from gray value of zero to 255. It is indicated that pixel gray value pair counts along the diagonal decrease while the number of off-diagonal gray value pairs increase with dispersion induced by misregistration. This effect is more clearly demonstrated when there exists a one-to-one correspondence in pixel gray values as depicted by Fig. 1 (middle row). In most cross-modality cases, as represented by Fig. 1 (bottom row), there exists a distinct pattern of pixel gray value correspondence. In both examples, misregistration is noted by characteristic dispersion in the histogram.

The corresponding MI is listed for each 2D histogram plot in Fig. 1, which illustrates the effect of misregistration. A plot of MI versus dx (in-plane lateral translation) of the T_1- and T_2- weighted MR image pair depicted in Fig. 1 (bottom row) is shown in Fig. 2. The global minimum (dx = 0) indicates the position where the two images are registered. MI approaches its lower bound when the two images are highly correlated and its upper bound when they are uncorrelated. The minimum MI for a given image pair is achieved when the geometric mapping produces the most correlated, i.e., registered, data sets, regardless of modality. Since MI is computed from the scatter plot of gray values, no gray level segmentation is required. Further discussions regarding the effect of 2D histogram binning and local minima on the MI optimization curve can be found in the earlier works (5,11).

Automated Registration

The registration process is an iterative method driven by MI cost metric and the Nelder-Mead downhill simplex optimization algorithm was implemented (12). The optimization routine determines the transformation coefficients for a coordinate mapping using three control points, e.g., rotate/translation, and performs trilinear interpolation to map gray scale values of the image voxels. The MI cost metric is computed from the voxel/pixel gray values in the reconstructed data set; therefore, the effect of the geometric mapping is manifested. Each optimization cycle is initiated by a random perturbation of the initial transformation vector. During the iteration, the optimizer moves the control points by small increments in an orderly fashion within the given radial bound. At each configuration of the control points, the data sets are mapped, and the resulting MI is computed and passed to the optimizer, which uses this information to compute the next control point configuration. The optimizer keeps a sufficient history of control point positions and MI values to allow it to move toward an optimal control point configuration. The trilinear interpolation process uses the original data set for each iteration instead of using the previous interpolation to generate the successive data. This approach prevents round-off and other undesired interpolation effects such as smoothing from accumulating across iterations. For the fMRI data sets, each iteration was set to stop when movement of control points is < 0.01 mm and the optimization cycle was repeated till the $\Delta MI < 0.00001$ for successive cycle.

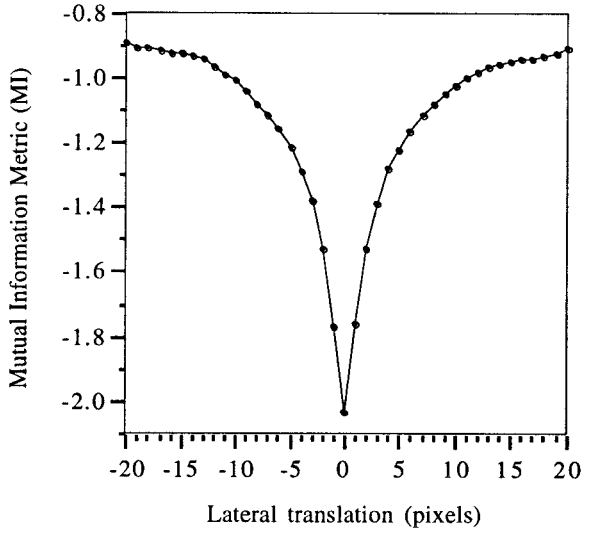

FIG. 2. A plot of MI versus lateral displacement in the range of $-20 \leq dx \leq 20$ pixels using the T_2- and T_1-weighted MR image pair as displayed in Fig. 1 (top and bottom row). The plot represents the optimization curve for the automated MI registration (2D histogram bin = 255), where the global minimum shows the point of register.

Map-Slice-to-Volume Approach in Motion Correction

The significance of this individual slice-based method is its adaptability to the multislice acquisition protocol, i.e., multislice EPI. Each slice in a time series fMRI data set was registered with the anatomical reference using the rigid body, a six DOF transform. The optimized transformation parameters, i.e., estimated motion parameter, were used for final reconstruction of each slice, in which the slice is reconstructed into a volume data in the same spatial coordinates as the reference volume (slice repositioning). The process is represented in Fig. 3 (top row) to illustrate that each slice is repositioned in a volumetric data set with which the statistical analysis is performed. In this manner, the process accommodates 3D random subject motion that occurs between each slice acquisition; i.e., motion is not restricted to a plane and each slice is handled independently from each other.

Slice-Stack Approach in Motion Correction

The automated registration routine is designed to be used for 2D, 3D, affine, and warping models. By using a slice stack from the time series fMRI data, i.e., slice-stack approach, the Statistical Parametric Mapping (SPM)-like mechanism was constructed. However, SPM approximately models slice-stack registration by using least square alignment, which cannot offer as accurate registration solution. (The volumetric registration presented in this study would be a valid method for data acquired using 3D *volumetric* fMRI sequence, i.e., multishot 3D EPI, to compensate for the movement between shots.) Each slice-stack from a time series fMRI data was registered with the anatomical reference volume and reconstructed using the same spatial extent as the reference volume. Figure 3 (bottom row) depicts motion correction methods employ-

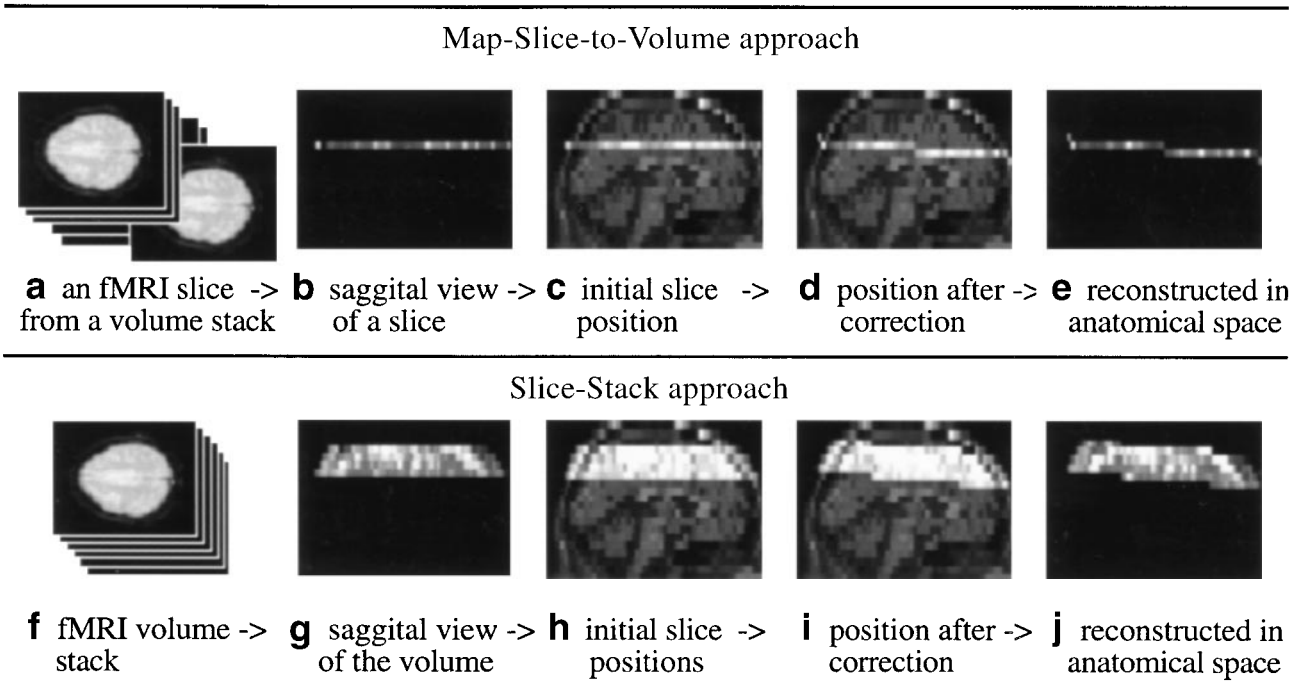

FIG. 3. Motion correction scheme depicting map-slice-to-volume (top row) and slice-stack (bottom row) approach by sagittal view of a brain. The far left column represents (**a**) an fMRI slice and (**f**) volume of stacked slices in an activation cycle. The next two columns show (**b**,**c**) the fMRI slice and (**g**,**h**) volume as positioned by the slice selection pulse during acquisition. Spatially corrected positions representing 5° rotation of head in saggital plane are shown for (**d**) the slice and (**i**) volume, and the last column presents reconstructed fMRI volumes from (**e**) the slice and (**j**) volume in the anatomical reference space. In the map-slice-to-volume approach, an individual slice is repositioned into the anatomical volume space as each is subject to different motion parameters and the procedure is repeated for each slice in a time series fMRI. In the slice-stack approach, accurate relocation of slices is compromised by overlooking the time interval between slices and assuming all the slices in one activation cycle are subjected to the same motion parameters.

ing the map-slice-to-volume and slice-stack registration approaches.

Nonparametric Statistical Analysis

The result of the map-slice-to-volume registration approach presents the statistical issue of variable sample size. The variability in subject motion is not assumed to follow any pattern or be in-plane; thus, voxels in the registered slice-fit-into-volumes in each activation cycle may not match in sample counts. The general approach of nonparametric statistical method using voxel-by-voxel random permutation was employed for significance testing of differences in voxel intensities in fMRI data. This approach provides simplicity and versatility of robust testing for each voxel independent of sample size variability (13).

The chosen test statistic is the averaged difference between activation and rest images in the time series. A sample of the intensity difference permutation distribution was obtained by 10,000 random draws of the data to attach a P value to the test statistic. Since under the null hypothesis of no activation, the result is independent of temporal ordering of the data, the time series data was shuffled in a random order to compute a new value of the test statistic based on a random pick. Shuffling the data repeatedly and generating a test statistic for each ordering generates the permutation distribution of the test statistic. Counting the number of values in this distribution that are greater than or equal to the true observed value of the test statistic obtained from the true ordering of the data and dividing by the number of simulated test statistics yielded an empirical P value for the test statistic. A good approximation to the exact permutation distribution was obtained by 10,000 random samplings from a uniform random number generator.

The random permutation test was performed at each voxel and the null hypothesis was tested with a single threshold, i.e., $P = 0.001$, to determine significance in a pair-wise subtraction value of voxel intensity. Voxels with sample size $N < 3$, as a result of registration, in either stimulus (on or off) half-cycle were ignored.

RESULTS

Functional Map From fMRI; Map-Slice-to-Volume Versus Slice-Stack Approach

Activation maps of individual subjects were produced by random permutation test of time series EPI ($P = 0.001$) after performing motion correction using map-slice-to-volume and slice-stack approaches. Figure 4 displays colorized statistical maps superimposed on the anatomical MRI used for registration of each time series EPI of two normal volunteers, (a and b), performing a motor task, uni-lateral sequential finger tapping. These are selected slices from 3D volumetric statistical maps to show activated regions. Significant voxels are marked in blue and red to indicate

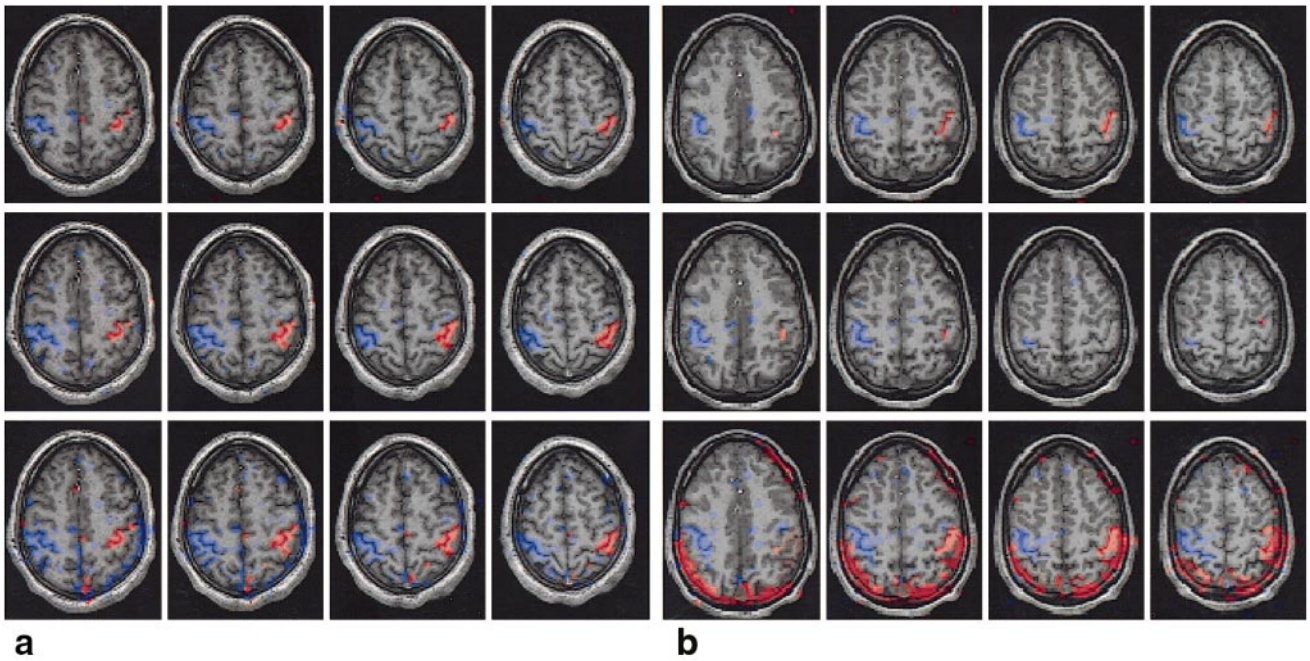

FIG. 4. Functional MRI of two normal volunteers, (**a** and **b**), performing the unilateral finger tapping task. Rows show statistical maps of time series EPI; bottom: without motion correction; middle: with slice-stack correction; top: with map-slice-to-volume correction, superimposed onto the T_2-weighted anatomical volume MRI of each subject. The two data sets show different levels of motion artifacts as indicated by signals presented in the periphery of the brains in uncorrected (bottom) data; the images in a show moderate motion artifacts while those in b show severe artifacts that complicate statistical inference of fMRI signal.

the temporal positive and negative correlations, respectively, in the uni-lateral activation cycle. In each data set, images in the bottom row represent statistical maps computed without any motion correction, the middle row represents maps calculated from images corrected by slice-stack registration and the top row shows maps from map-slice-to-volume correction. The maps from the uncorrected data set show the characteristic motion-related false activation voxels around the periphery of the brains. In both the map-slice-to-volume and slice-stack correction analysis method, the images show the absence of gross motion effect that is evident in the maps of uncorrected data.

The improved performance of the map-slice-to-volume approach is well demonstrated in the data set shown in Fig. 4b, which displays more severe motion artifacts than the data in Fig. 4a, causing significant false activation in the statistical maps without correction. The figure illustrates that the slice-stack correction method exhibits the inherent shortcomings that apparently invalidate the statistical inference when subject motion artifact is prominent in a multislice fMRI data set. Improved *sensitivity* of map-slice-to-volume motion correction is indicated by the presence of high-intensity (colored) voxels inferred as activated voxels common to both subjects, and reduced random activation signifies improved *specificity* compared with the slice-stack registration. The improved performance of the map-slice-to-volume method is due to repositioning the activation data into the actual geometric loci.

Performance Evaluation of Map-Slice-to-Volume Registration

The automated motion correction routine selects a slice image from time series data (295 slice images, for three cycles) and finds a spatial location in the anatomical reference by rigid-body transformation. The resulting registration parameters are used to reconstruct the slice in the anatomical volume space, i.e., each slice turns into a volume in this map-slice-to-volume approach. The routine repeats the process for each slice in the time series. Registration and processing were performed using Advanced Visualization System (AVS/5) on a DEC Model 3000/500x Alpha workstation running under OSF/1. Each slice registration took an average of 15 sec.

Accuracy Evaluation of Map-Slice-to-Volume Registration

Errors in the map-slice-to-volume registration technique were assessed using simulated MRI data in correction of out-of-plane and in-plane subject head movements. The simulated T_1- and T_2- weighted MRI data were downloaded from the web site of the International Consortium of Brain Mapping (ICBM) at the Montreal Neurological Institute, McGill University (14). The two data sets are in complete geometric register and therefore provide the known truth. The volumes of the simulated data sets are in 1 mm isotropic resolution in Talairach space. A slice from T_2-weighted MRI volume, downsized and low-pass filtered to match the resolution of fMRI data, $4 \times 4 \times 8$ mm voxel size, was registered into the T_1-weighted volume data used as a

Table 1
Assessment of Registration Accuracy*

	Rotation (°)		
	$\Delta\theta_X$	$\Delta\theta_Y$	$\Delta\theta_Z$
Mean	−0.0211	−0.1030	0.0712
SEM	0.0390	0.0681	0.0337
P value	0.5834	0.1452	0.0532
	Translation (mm)		
	Δx	Δy	Δz
Mean	0.0558	−0.0710	−0.0024
SEM	0.0372	0.0273	0.0310
P value	0.1478	0.0229	0.9380

*Transformation parameters from registration of a slice into the anatomical reference volume using simulated MRI data were analyzed by the mean and standard error of the mean (SEM) of difference from the truth, and *P* value from *t* tests for statistical significance. A slice from the simulated T_2-weighted MRI data was registered into the T_1-weighted volume. The values are calculated from the results of 10 optimizations initialized with the same control points. The optimization parameters, radial bound (10 mm) and the stopping criteria (0.01 mm), were consistent with the optimization of the experimental data.

reference volume. The registration process was repeated 10 times, each initiated with a random displacement of the control points. The resulting transformation parameters, rotation, and translation in three coordinate axes from 10 registrations were analyzed with respect to the known truth for the evaluation of registration accuracy.

The two simulated MRI data sets are created to be in completely registered position and the final result of aperfect registration would yield translational and rotational parameters of zero. Transformation matrices from the slice registration were analyzed to assess the accuracy and range of in-plane and out-of-plane components. The errors in registration of the simulated T_1- and T_2- weighted MRI images were assessed by mean displacement of the registration parameters with respect to the truth, the identity transformation. The mean and standard error of the mean (SEM) are listed in Table 1. *P* values were calculated from t tests for statistical significance of the differences in transformation parameters from the truth. The result shows that the subvoxel accuracy of the registration parameters is in the range of -0.10 ± 0.07°, and -0.07 ± 0.03 mm (mean ± SEM), in maximum rotation and translation, respectively, where the voxel resolution is 1 mm^3 for the reference (T_1-weighted) MR image. Consistently, t tests show that the errors are not statistically significant at the 0.05 level when tested against zero transformation parameters with the exception of the translation in Y, which, however, shows very small values of the mean and SEM.

Motion Parameters From Time Series EPI

The range of motion was analyzed for the time series fMRI of a normal volunteer performing the uni-lateral motor task, whose statistical map is presented in Fig. 4b. Listed in Table 2 are the mean and SEM of the motion parameters, in rotation (°) and translation (pixels), determined for two axial slices positioned at superior (sup) 22.8 and 30.8 mm. In addition, the minimum and maximum values listed present the range of the subject motion. The slice that was positioned closer to the superior edge (sup 30.8 mm) exhibits wider range of motion.

Anatomical Standardization of the fMRI Signal

The resulting functional signal was transformed into standard anatomical coordinates using a normal brain model provided by the ICBM, which is defined in 1 mm voxels in Talairach space. The purpose of the transformation is to demonstrate the validity of motion correction process by localization of fMRI signal in a common coordinate system to relate data across different individuals. The anatomically standardized functional map was obtained by volumetric registration of the patient's anatomical MRI into the ICBM space using an affine transformation of seven DOF, i.e. rotation, translation, and isotropic scaling. The augmentation of DOF to seven is an essential step since it is evident that the limited geometric functions with rotate-translate transform cannot handle the scale offset in the cross-subject anatomical mapping. Non-linear transformations involving higher DOF, i.e., warping, for more comprehen-

Table 2
Range of Movement Parameters Determined by Registration of Individual Slice Images From the Time Series fMRI Data Into the T_1-Weighted Anatomical Reference Volume*

Rotation (°)	Slice location at sup 22.3 mm			Slice location at sup 30.3 mm		
	θ_X	θ_Y	θ_Z	θ_X	θ_Y	θ_Z
Mean	0.6954	0.1468	0.4063	0.3937	0.7060	−0.7107
SEM	0.0804	0.0875	0.1094	0.1005	0.3329	0.2519
Min. rotation	−0.6182	−1.2231	−2.3213	−2.2287	−13.5825	−9.6233
Max. rotation	2.1370	1.5936	2.1889	3.0724	2.7655	7.3875
Translation (mm)	X	Y	Z	X	Y	Z
Mean	−2.2501	0.9334	1.0279	−2.1889	1.3514	0.6544
SEM	0.0366	0.0588	0.0984	0.0490	0.0996	0.3244
Min. translation	−2.7737	−0.7077	−0.5446	−3.0045	−0.5844	−1.2331
Max. translation	−1.6106	1.6644	2.6391	−0.7513	4.1750	14.4742

*The motion parameters were determined for the data set shown in Fig. 4b. Two slices were analyzed to represent two axial slice locations. The slice at the more superior position (sup 30.3 mm) exhibits wider range of movement.

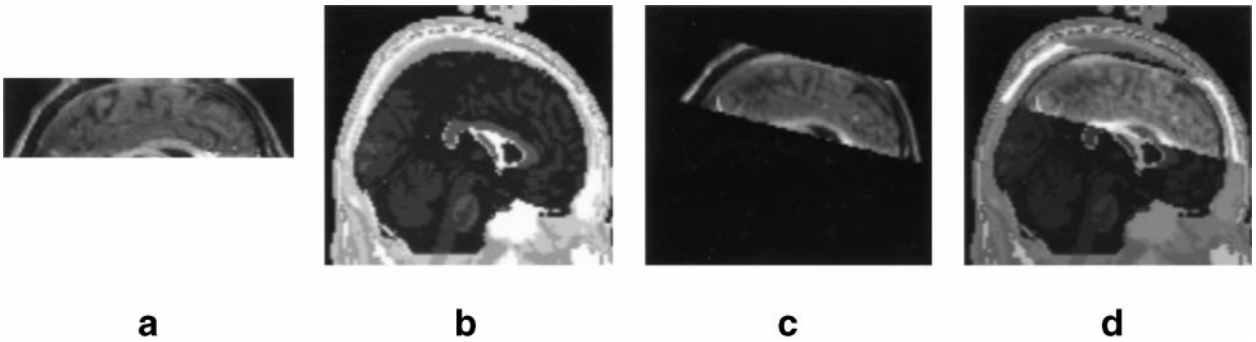

FIG. 5. Transformation of an anatomical T_1-weighted MR volume data (**a**) to the ICBM anatomical model of normal brain (**b**) is depicted in a sagittal view. The transformed MR volume (**c**) is superimposed (**d**) on the standard brain model for visual presentation of the match.

sive cross-subject anatomical mapping are not considered in this work (15). The resulting parameters were used to transform the volumetric statistical map of fMRI data. Anatomical MRI volume covering superior portion of a subject head transformed into the standard ICBM brain model is displayed in Fig. 5. In Fig. 6, sagittal views of the functional images from the two data sets are displayed as superimposed on the anatomical volumes and registered in the standard coordinate system. The two lines in each image indicate the same slice positions of the upper and lower limits of the volume from which the axial slices are displayed in Fig. 7. Localization of fMRI signal in a standard brain atlas, i.e., ICBM, is displayed in Fig. 7.

The two data sets from the normal volunteers performing the uni-lateral finger tapping task show consistent significant voxel locations in common regions known to be associated with the cortical motor stimulation.

DISCUSSION

This paper demonstrates the accuracy and reliability of the map-slice-to-volume approach in motion correction of time series fMRI data set acquired by multislice EPI. The results suggest improved detection and localization of functional signals across subjects exhibiting mild to moderate motion. Results of analyses of fMRI data from a primary motor task using map-slice-to-volume and slice-stack methods are presented in comparison with the uncorrected data analysis.

Analysis of time series fMRI acquired by multislice EPI using an SPM-like method, i.e., slice-stack correction, introduces additional registration errors based on the false assumption that there is no relative movement between slices (1). The slice-stack retrospective motion correction would be valid for multi-shot volumetric EPI acquisitions (16,17). The inadequacy of the slice-stack motion correction is documented in our result in Fig. 4 showing the statistical maps from two normal subjects. Images in Fig. 4a exhibit less motion artifacts than those in Fig. 4b, and thus the slice-stack correction presents reasonable statistical map compared with the ones from the map-slice-to-volume method. However, when dealing with the fMRI data exhibiting more severe motion artifact as presented in images in Fig. 4b, only accurate repositioning of each slice relative to the anatomical reference volume leads to the meaningful statistical inference of the functional signals.

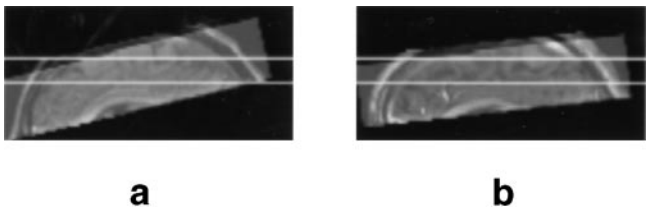

FIG. 6. Sagittal view of the functional map superimposed on anatomical volume in standard ICBM coordinates. The data sets (**a** and **b**) are the ones used in Fig. 4. The two lines in each image indicate the same slice positions.

The result of the fMRI signal analysis via motion correction is presented in a standard coordinate system. The transformation process using seven DOF was used to locate spatially acquired MRI volume data of individual subjects in a common coordinate system. Anatomical standardization of functional signals is used to relate localization of functional activation across subjects using a common coordinate system. Since the anatomy of the cerebral cortex varies significantly between individual brains, there have been extensive studies for inter-subject brain warping to standardize individual brains relative to a common coordinate system (15). However, for our purpose, simple registration using rotate/translate/iso-scaling is used to standardize the orientation of slice selection in each acquisition process. The result demonstrates fMRI signals localized at consistent slice locations between the two normal subjects.

A nonparametric statistical test using random permutation is employed for its robustness and its independence of underlying distribution assumption. A voxel-by-voxel random permutation test is performed based on a predefined set of images in each cycle assuming a delay of approximately 6 sec, i.e., three images, for hemodynamic response. Calculation of a statistical map using 10,000 random permutations of fMRI volumes in a $64 \times 64 \times 5$ image matrix required roughly 25 min. For a more efficient statistical test, however, empirical characterization of both spatial and temporal covariance would be prudent.

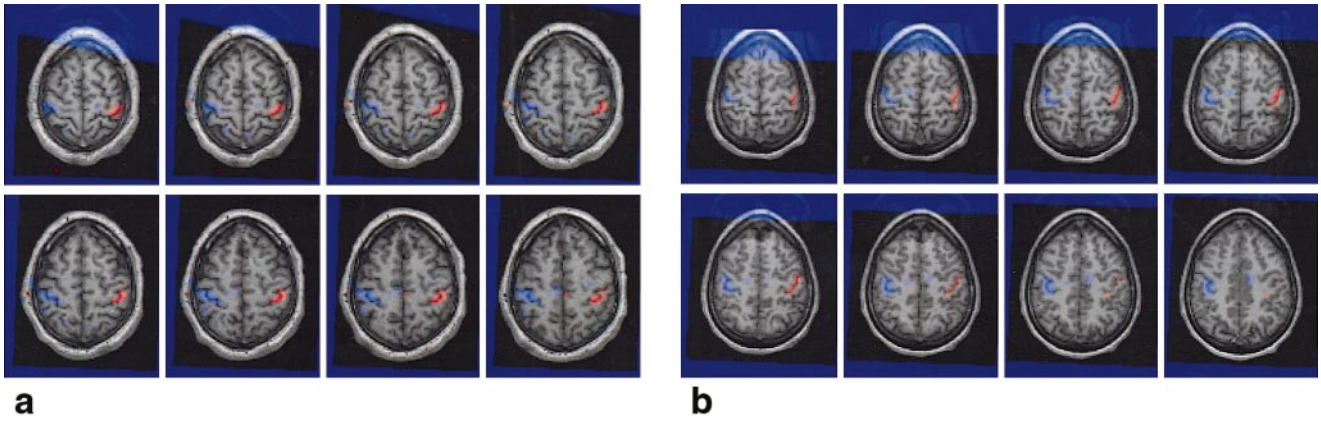

FIG. 7. Slice images of the transformed statistical volumes superimposed onto the anatomical volumes are displayed. The images are from the same data sets presented in Fig. 4. The images display the functional maps from the two normal volunteers superimposed on the anatomical volume in the standard ICBM brain coordinate system. Axial images of the superimposed data are displayed in (**b**) as slices were from the volume, where the upper and lower limits are indicated by the high-intensity lines in the sagittal view (**a**). As the two volumes are in the standard anatomical space, the axial images (b) are from the identical slice locations, at every 2 mm between sup 46 and 60 mm.

Implementation of retrospective image registration for motion correction of fMRI data has been critiqued based on the results from the least square slice-stack realignment method followed by parametric statistical analysis as provided in the SPM software package (18). Our result presents evident improvement in fMRI signal detection by employing map-slice-to-volume motion correction furnished by nonparametric statistical analysis suited for multislice fMRI time series data. Acquisition sequence-induced artifacts may affect performance of MI-based registration applied to fMRI motion correction. Echoplanar functional magnetic images are susceptible to localized image distortion arising from cardiac and respiratory pulsation as well as local magnetic field change. Motion correction using non-linear warping may be necessary to correct deformations caused by cardiac-induced acceleration in which gating is impractical. In addition, field inhomogeniety correction has been identified as a leading factor in accurate registration (19,20). The prospect of generating an accurate functional map from fMRI using retrospective correction will be greatly enhanced as the motion correction method matures to accommodate these acquisition-dependent variables in fMRI.

Our map-slice-to-volume correction method has been applied for analysis of primary motor task fMRI data that provide the most robust and repeatable signal enhancement across subjects. Accuracy and reliability of this method would be substantially beneficial for analyzing more complex functional paradigms that may involve wider spatial distribution of functional signal and are more susceptible to motion artifacts, e.g., working memory or speech. Such algorithm may allow fMRI to be used as clinical tool for patients with significant motion disorders, i.e., Parkinson's disease. Currently, patients with significant motion disorders are often excluded as likely candidates for fMRI exams. Development of an effective retrospective motion correction method would be invaluable, especially for data sets acquired, without the benefit of specialized hardware, from patients with motion deficit and whose function response test is impaired by the motion artifacts.

REFERENCES

1. Friston KJ, Ashburner J, Frith CD, Poine JB, Heather JD, Frackowiak RSJ. Spatial registration and normalization of Images. Hum Brain Map 1995;2:165–189.
2. Hajnal JV, Mayers R, Oatridge A, Schwieso JE, Young JR, Bydder GM. Artifacts due to stimulus correlated motion in functional imaging of the brain. Magn Reson Med 1994;31:289–192.
3. Hu X, Le TH, Parrish T, Erhard P. Retrospective estimation and correction of physiological fluctuation in functional MRI. Magn Reson Med 1995;34:201–212.
4. Bullmore E, Brammer M, William SCR, Rabe-Hesketh S, Janot N, David A, Meller J, Howard R, Sham P. Statistical methods and estimation and inference for functional MR image analysis. Magn Reson Med 1996;35: 261–277
5. Kim B, Boes JL, Frey KA, Meyer CR. Mutual information for automated unwarping of rat brain autoradiographs. Neuroimage 1997;5:31–40.
6. Meyer CR, Boes JL, Kim B, Bland PH, Zasadny KR, Kison PV, Koral K, Frey KA, Wahl RL. Demonstration of accuracy and clinical versatility of mutual information for automatic multimodality image fusion using affine and thin plate spline warped geometric deformations. Med Image Anal 1997;3:195–206.
7. Cover TM, Thomas JA. Elements of information theroy. New York: John Wiley & Sons; 1991.
8. Wells WMI, Viola P, Atsumi H, Hakajima S, Kikinis R. Multimodal volume registration by maximization of mutual information. Med Image Anal 1996;1:35–51.
9. Viola P, Wells WM. Alignment by maximization of mutual information: Proceedings of the 5th International Conference on Computer Vision, MIT, 1995. IEEE 95CH35744 p 16–23.
10. Collignon A, Vandermeulen D, Suetens P, Marchal G. 3D multimodality medical image registration using feature space clustering. Lecture Notes Comput Sci 1995;905:195–204.
11. Kim B, Boes JL, Frey KA, Meyer CR. Mutual information for automated multimodal image warping. Lecture Notes Comput Sci 1996;1131:349–354.
12. Press WH, Flannery BP, Teukolsky SA, Vetterling WT. Numerical recipes in C: the art of scientific computing.'' Cambridge: Cambridge Press; 1998. p 305–309.
13. Good P. Permutation tests. New York: Springer-Verlag; 1994.
14. Cocosco CA, Kollokian V, Kwan, RK-S, Evans AC. Brain Web: online interface to a 3D MRI stimulated brain database. Neuroimage 1997;5: S425.

15. Meyer C, Boes JL, Kim B, Bland PH, Frey K. Warping normal patients onto the ICBM atlas by maximizing MI. Neuroimage 1998;7(4):S724.
16. Mansfield P, Howseman AM, Ordidge RJ. Volumar imaging using NMR spin echoes: echo-volumar imaging (EVI) at 0.1 T. J Phys E 1989;22:324–330.
17. Song AW, Wong EC, Hydge JS. Echo-volume imaging. Magn Reson Med 1995;32:668–671.
18. Lee CC, Grimm RC, Manduca A, Felmlee JP, Ehman RL, Riederer SJ, Jack CR, Jr. A prospective approach to correct for inter-image head rotation in fMRI. Magn Reson Med 1998;39:234–243.
19. Meyer CR, Bland PH, Pipe J. Retrospective correction of intensity inhomogeneities in MRI and CT. IEEE Trans Med Img 1995;14:36–41.
20. Kim B, Boes JL, Bland PH, Meyer CR. Effects of inhomogeneity correction on mutual information based image registration. In: Proceedings of the ISMRM Fifth Annual Meeting. Vancouver, Canada, 1997. p 2019.